

ANALYSIS OF THE STATIC BEHAVIOR OF THE SHAFT BASED ON FINITE ELEMENT METHOD UNDER EFFECT OF DIFFERENT VARIANTS OF LOAD

Aleksandar Ašonja^{*1}, Eleonora Desnica², Ivan Palinkaš²

¹Faculty of Economics and Engineering Management in Novi Sad, University Business Academy in Novi Sad, Serbia

²University of Novi Sad, Technical Faculty "Mihajlo Pupin", Department of Mechanical Engineering, Zrenjanin, Serbia

Abstract:

By using the method of finite elements and starting with the possibilities given by the program system ANSYS in the field of application, research has been performed regarding the analysis of static behavior of a centrifugal pump shaft. The computational analysis of static behavior of shaft using the method of finite elements on the examined model during the phase of projecting, was aiming for a timely sighting of critical spots, in order to avoid possible further malfunction. In this way it is possible to examine validity of the basic solution with no need for making the prototypes. By static behavior analysis, in other words, using the method of finite elements it was shown to which extent can certain conditions of exploitation, created tensions, that is shifted knots, cause difficulties in the whole model performance. Analysis of the static behavior of shaft was performed for two cases with different load: the effect of radial force and the torsion moment. A special attention was given to modelling of rolling-element bearings and following of their condition in relation to outside influences.

ARTICLE HISTORY

Received: 09 February 2016

Accepted: 28 February 2016

Available online 30 June 2016

KEYWORDS

FEM analysis,
shaft,
load tension,
model

1. INTRODUCTION

The Finite Element Method (FEM) is a procedure for the numerical solution of the equations that govern the problems found in nature. Usually the behaviour of nature can be described by equations expressed in differential or integral form. For this reason the FEM is understood in mathematical circles as a numerical technique for solving partial differential or integral equations. Generally, the FEM allows users to obtain the evolution in space and/or time of one or more variables representing the behaviour of a physical system [1].

Mechanical analysis, as an integral segment of engineering analysis [2], includes software procedures which in an automated regime enable performance of mechanical (static, kinematic and dynamic) analysis of examined models in conditions that relate to exploitation conditions [3].

Due to complexity of analytical procedure of shaft static analysis, with its bearings, and the need for a more comprehensive analysis of geometry influence, conditions of load and other external influences, in this paper we shall use the adequate method of numerical analysis.

The FEM which will be used in this paper belongs to a group of contemporary numerical methods which are being used with very complex formations and other circuits which have a great static uncertainty, and are also exposed to complex strain. The FEM is based on solving a system of a large number of algebraic linear equations in a matrix form.

The basic idea of the FEM consists of dividing the continual mass 2D or 3D model to discrete (finite) elements [4]. The method used in this paper belongs to methods of discrete analysis, by which the continuum (geometry) of a material is divided to a strain of sufficiently small elements

which are finite and represent an approximation of the real continuum.

Contemporary methods FEM provide faster calculations of tension and deformations caused by external forces, heating, disrupted thermal and other dilatations. During that the form and dimensions of the model can be varied in order to gain a high degree of mass rationality, high working reliability, and especially accuracy of the calculation results [5]. Today these methods are mostly employed in industry of machine building, airplane industry, construction, military industry, cosmotronics, nuclear technology, production of home appliances, agricultural machines, tools, accessories, vehicles etc. [6].

The justification of this study is based on the fact of low reliability of certain mechanical transmissions are, for example, agricultural cardan shafts [7-10]. Research of numerical analysis and correction in changing the geometry of the cross shaft can lead to a significant reduction of critical stress [11]. Similar studies of analysis of the static and dynamic characteristics of composite shafts are shown in the works of [12,13].

2. ANALYSIS OF SHAFT BY APPLICATION OF FEM UNDER STATIC CONDITIONS

Analysis of static behavior by using the software system ANSYS R5.4 was performed on the shaft of a centrifugal pump, figure 1. The named analysis will be performed for loads which consist of:

- effect of radial force between two bearings and
- rotary moment at the shaft's beginning.

Modeling and analysis of static behavior of the shaft will be conducted in a concrete case by a specified procedure which will be performed through following phases:

- modeling of the pump shaft;
- discretization of the geometric model;
- discretization of the geometric model by the network of finite elements;
- definition of boundary conditions and load;
- processing - solving of the set mathematical model; and
- presentation of the calculation results in numerical and graphic form.

By graphic presentation of the state of the analyzed model the following presentations will be given:

- contour (in which the changes of characteristic shifts and tension will be

shown on the whole model, with the borders between neighboring areas presented in continuous lines);

- the deformed model under the effect of load; and
- reaction forces on the model.

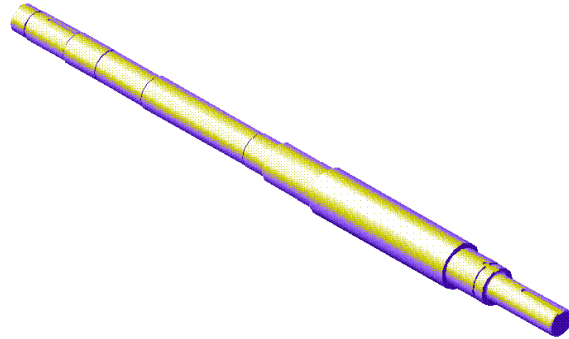


Fig. 1. The model of the shaft shown in 3D

2.1. Modelling of the shaft

Building of the database on the pump shaft enables forming of a discretized model on which different loads and boundary conditions can be set upon, which gains shortening of processing time and of the analysis time itself. In the concrete case, generating the network of finite elements will be performed with tetrahedral elements, which can pretty good describe the rotation form of the observed model. Using the method of volume modeling, building of the model of the pump shaft will be performed by the method for computational generating of the volume model, which is by rotation of the profile round the symmetry axes (sweeping). Selected finite elements will be connected in knot points which represent imaginary knot bonds. For each knot point where the finite elements will be connected, there will be set an equation of elastic forces which define the relation between tension and deformation. The balance of finite elements is analog to the balance of sticks in a grid carrier. External load and limitations are included in equations for finite elements on the contour of the form and by solving the system of these equations values of shifting are obtained, that is deformation and "von Mises's" tensions in all knot points. After calculating, extreme values of tension, that is extent of shifting of the knots along the Y axes, will be shown both graphically and numerically.

Based on the analysis of the possibilities of the software system ANSYS for this concrete case of shaft there has been concluded that the modeling

was most easily performed by rotation of the profile of the upper half of the axial section around the rotation axes by 360°. Compared to the real form of the shaft, its modeling was performed in the way of omitting downcast edges, groove and radiuses. However, at a later phase of generating the network of finite elements there has been performed grouping of selected contours due to problems in calculating, based on which a simplified profile was obtained shown on figure 2 with representation of coordinate points of the given contour. Beside the defined points of the contour of the shaft's half-section, in the coordinate system X-Y in the figure 2 points (1-20) are also defined, which define the shaft model.

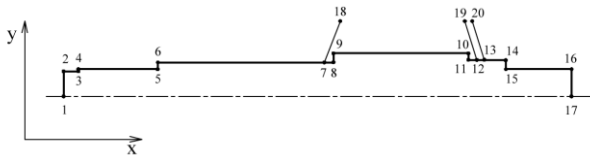


Fig. 2. Final simplified layout of the shaft with keypoints of the upper half of the shaft's axial section profile

2.2. Discretization of the geometric model

Finite element analysis (FEA) with standard methods requires the discretization of the physical domain into a finite element mesh, whose boundaries conform to the boundaries of the geometry [14]. The way of discretization, selection of type and number of elements as well as the number of knots depended on the nature of the problem in matter and the required accuracy of the solution. Generally, the accuracy of the solution increases with the increase of number of elements and knots, but it causes increase of the total working time. If only the shifting is examined, MFE requests even a smaller number of defined knots, however if a detailed analysis of structure's tension state is being performed it is necessary to increase the network density in the load area.

The analyzed model is discretized by using the option of automatic generating of the network (free meshing), based on which the network of 13,032 knots and 6816 elements was discretized. Basic parameters that characterized the component of the 3-D model of the shaft consisted of: 290 keypoints, 497 lines, 272 areas and 16 volumes.

2.3 Discretization of the geometric model by a network of finite elements

Each finite element is characterized by the: shape of the element, number of knots, number of

degrees of freedom in each knot and the type of interpolation functions. Depending on these parameters, elements that are at ANSYS disposal can be: one-dimensional, two-dimensional and three-dimensional, as well as with linear, square and cubic interpolation.

For discretization of the model generated in the previous phase, a 3-D volume finite element *Solid 72* of the parabolic tetrahedron type was used. Basic characteristics of this finite element were four knots and the following degrees of freedom: 3 (UX, UY, UZ), 3 (ROTX, ROTY, ROTZ). For discretization of the line that substitutes rolling elements of the ring ball one-lined bearing 6212 and the ring ball two-lined bearing with a slantwise contact 3311, the 2-D finite elements *Link 11* of the spring with loss type were used figure 3. Basic characteristics of this finite element were two knots and the following degrees of freedom 3 (UX, UY, UZ).

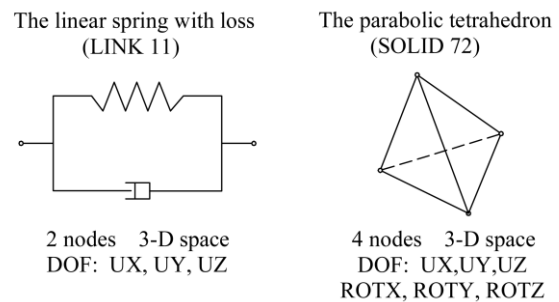


Fig. 3. Graphic symbols of the used finite elements Link 11 and Solid 72

After forming an adequate discretized model of bearing, there have been examined possibilities of implementation of suitable software which is based partially on linear elasticity theory equations. For selected values of load and defined boundary conditions, using the iterative procedure there were obtained approximate values of shifting and tension of individual parts of ball bearing (in numeric and graphic form).

2.4. Defining boundary conditions and load

In the first case of the shaft load under radial force, it was also considered the influence of shaft's own weight, that is, the gravity force.

In the second case of the shaft load the analyzed shaft receives, in the front left part through the junction with a brim IEC 21.220.10, the rotation moment from the electric motor's shaft and transmits it to the turbine housing. During the transmission of force the shaft is exposed to torsion moment at the junction spot.

The volume model of the shaft is linearly distributed regarding the X axes, while the linear springs are conically distributed over the spots where the pellets are leaning. Boundary conditions of linear spring should meet following presumptions:

- limited shift of the knots in elastic supports at the joint along the shaft edge, except the axial direction; and
- limited shift of the knots in elastic supports at the end of elastic springs.

Based on the presented, at the spot of the knots of the linear spring bearing 6212 and 3311 which are situated on the shaft edge, two degrees of freedom along X and Z axes are deducted, while shifts along Y axes are allowed. The knots at the free ends of springs have been deducted all three degrees of freedom. The Fig.4 shows bearings with given boundary conditions.

Beside the torsion, the shaft is during work exposed to the effect of radial force of 3000 N, which acts in the middle between two bearings, bending the shaft as shown in the figure 7.a. Other values of the calculated factors important for further analysis are: value of the force per every knot of 333.33 N, number of revolutions of the shaft of 2950 min⁻¹, power of 30 kW, rotation moment at the junction of 97.4 Nm, moment per every knot of 1106.8 Nm and angular velocity of 308 rad/s.



Fig. 4. Discretized bearings on the shaft with given boundary conditions

Formed geometric models of bearings construction represent grounds for further research of elastodeformation values in the bearing. However, in order to precisely determine values of contact tension and deformations, by which also elastic shifts, it is necessary to firstly define adequate parameters of the load distribution. The procedure of determination of external load of the bearing rolling bodies itself implies defining appropriate reactions of the bearing at the given load, that is: with which radial

and axial forces and moments the bearing reacts to the external loads, how many rolling bodies participate in the transmission of the load, what is the distribution of forces on the coupled bearing parts etc. In order to successfully solve this problem, previously are defined non-linear connections between static and kinematic parameters at contact strains.

Calculation of load distribution at ball bearings is rather specific, due to occurrence of contact non-linearity. Unlike non-linearity of geometry and material characteristics, contact non-linearity is conditioned by change in contact surface under effect of external load. The scheme of bearing load distribution, disregarding elasticity of the shaft and bearing housing, is given in figure 5. At ball bearings with slantwise contact, the following equation is applied [5] Eqn 1:

$$F_o = \frac{4,37 \cdot F_r}{z \cdot \cos \alpha} \quad (\text{N}). \quad (1)$$

Taking that the load of some rolling bodies F_i is variable in dependence on his relative square distance from F_o , equal Eqn 2:

$$F_i = F_o \cdot (\cos(i \cdot \gamma))^{\frac{1}{x}}, \quad (\text{N}), \quad (2)$$

where

$$x=2/3. \quad (3)$$

Assuming that the radial rigidity is not changed by change in angle γ , total shift in the place of rolling bodies caused by effect of radial force, can be determined based on Eqn 4:

$$\delta_i = \frac{F_i}{C_r} \quad (\mu\text{m}). \quad (4)$$

Shift components along Y and Z axes, δ_{yi} and δ_{zi} according to Eqn 5 and 6 are:

$$\delta_{yi} = \frac{F_{yi}}{C_r} \quad (\mu\text{m}), \quad (5)$$

$$\delta_{zi} = \frac{F_{zi}}{C_r} \quad (\mu\text{m}), \quad (6)$$

when their shift forces F_{yi} and F_{zi} are given in Eqn 7 and 8:

$$F_{yi} = F_i \cdot \cos \gamma \quad (\text{N}), \quad (7)$$

$$F_{zi} = F_i \cdot \sin \gamma \quad (\text{N}). \quad (8)$$

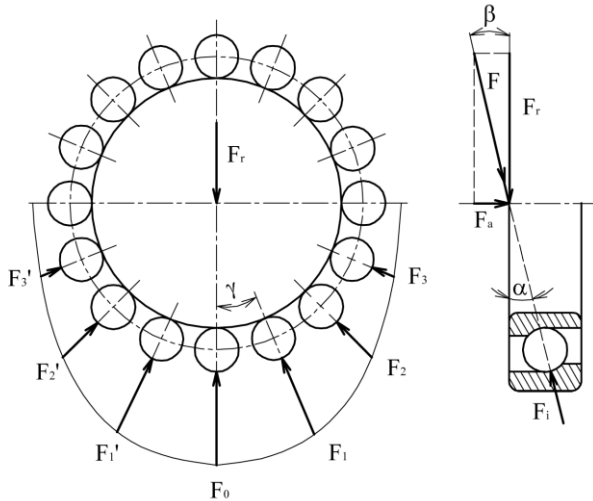


Fig. 5. The scheme of bearing load distribution

Examination of static behavior of shaft using the software system ANSYS aimed to establish its static rigidity, since it is a parameter that directly affects the bearings. In this paper the influence of bearing on the shaft was simulated by adding radial and axial rigidity to knots of finite elements network which are situated at the spot of bearing, figure 6. If total radial and axial rigidity of the bearing are known, rigidity of one spring element can be calculated according to Eqn 9 and 10 [15]:

$$C_r = \frac{C_{ru}}{z} \quad (\text{N}/\mu\text{m}), \quad (9)$$

$$C_a = \frac{C_{au}}{z} \quad (\text{N}/\mu\text{m}). \quad (10)$$

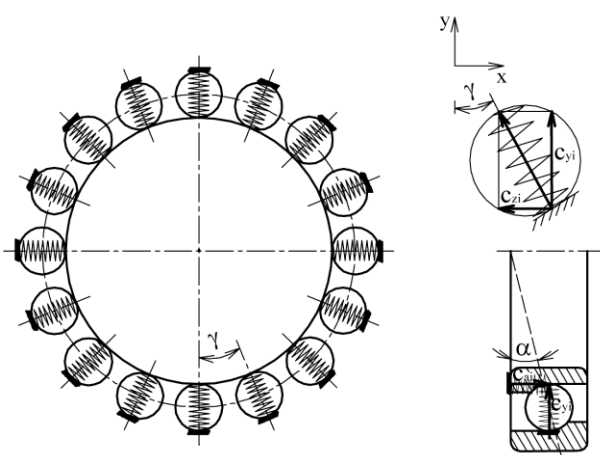


Fig. 6. Method of giving additional rigidity to finite elements network knots

Rigidity of single spring elements C_{yi} , C_{zi} and C_{ai} can further be calculated according to Egn 11, 12 and 13:

$$C_{yi} = C_r \cdot \cos \gamma \quad (\text{N}/\mu\text{m}), \quad (11)$$

$$C_{zi} = C_r \cdot \sin \gamma \quad (\text{N}/\mu\text{m}), \quad (12)$$

$$C_{ai} = \frac{C_a}{z} \quad (\text{N}\mu/\text{m}). \quad (13)$$

2.5. Processing of the given mathematical model

After the phase of generating the pump shaft's volume model, its discretization, calculation and setting the boundary conditions, the phase of setting a system of equations follows by using suitable processors, solvers. Having in mind that at generating the volume model of the shaft the points' coordinates were expressed in meters, it was necessary to adjust other characteristic parameters also, to preserve compliance of the used units system. Therefore, the following data connected to the very model of the shaft was used: shaft material (42CrMo4), elasticity module $E=2.17 \cdot 10^5 \text{ N/mm}^2$, specific density of the material $\rho=7.85 \cdot 10^{-6} \text{ kg/mm}^3$, sliding module $G=0.85 \cdot 10^5 \text{ N/mm}^2$ and Poisson's coefficient $\mu=0.3$. Chemical composition of the analyzed shaft's material is of: 0.42 C, 1.10 Cr and 0.25 Mo and can be classified as alloyed steel for low working temperatures. Maximal hardness of the steel used to make the shaft is 241 HB, plasticity limit is 800 N/mm^2 and the tensile hardness $900\text{-}1100 \text{ N/mm}^2$.

Based on the form of the shaft model and the number of bearings on the shaft of the pump, rigidity for single springs (pellets are identified with springs of specific rigidity) have been calculated. Calculated radial rigidities for single springs of the shaft were: in the first bearing $C_r=16 \text{ N}/\mu\text{m}$ and for the second and third bearing $C_r=10 \text{ N}/\mu\text{m}$.

3. RESULTS OF THE STATIC CALCULATION OF THE SHAFT LOAD

Analysis of the static behavior of the shaft based on the MFE under effect of different variants of load shown in this paper was used for obtaining a more comprehensive picture of a mutual relation between the shaft and the bearing, as well as the influence on the duration of the entire circuit.

Results of the analysis of static behavior of the pump shaft for both variants of load are shown in the figure 7, 8 and 9. It also states the largest shifts of the characteristic knots and the largest tensions in characteristic sections. The graphic part of the results presentation consists of illustrations of distribution of the equivalent tensions in the elements of the discretized model, shift of the knots along Y axes, as well as deformations in the elements of the discretized model.

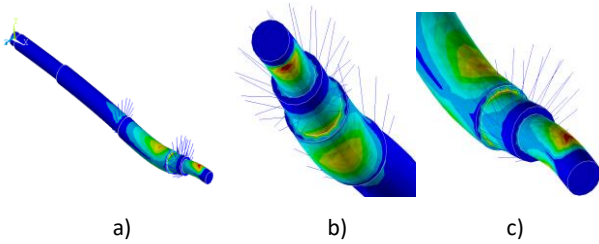


Fig. 7. Equivalent tensions on the shaft exposed to gravity and radial force; a) view in isometry, b) view in isometry at the spot of turbine blade from the lower side and c) view in isometry from the upper side

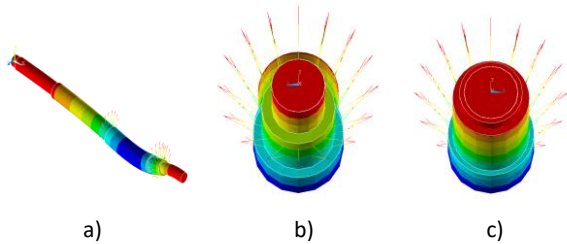


Fig. 8. Shift of the shaft knots along Y axes of the discretized model; a) view in isometry, b) view in isometry at the spot of turbine blade and c) view at the junction spot

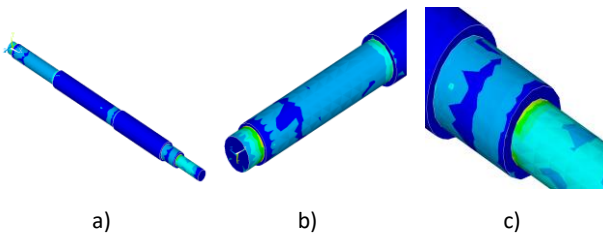


Fig. 9. Equivalent tensions at the shaft exposed to torsion moment; a) view in isometry, b) view at the junction spot and c) view at the spot of the two-lined bearing

4. DISCUSSION OF THE STATIC ANALYSIS OF THE SHAFT STATE

From the standpoint of equivalent tensions, in the first case of load under effect of radial force at the radius $\Phi 67$ mm part of the shaft between two

bearings, the largest equivalent tension of $\sigma_{ekv}=9.056$ MPa was registered at the knot 1655, that is at the $\Phi 40$ mm where the turbine blades are, figure 7.b. At the same cross section, but at the upper side at the knot 410 figure 7.c, the tension value is somewhat smaller and it is $\sigma_{ekv}=8.855$ MPa. At the force effect spot, the value of the tension in the knot 385 was $\sigma_{ekv}=0.745$ MPa, figure 7.c, that is its value at the same section but on the lower side in the knot 1628 is substantially higher and reaches $\sigma_{ekv}=6.805$ MPa, figure 7.b. Apart from these equivalent tensions there are also substantial local tensions at the spot of the ring ball one-lined bearing, with the value range $\sigma_{ekv}=1.378\div 1.475$ MPa, Table 1, and are situated in the knots 281 and 161, figure 7.a. Tensions at the ring ball two-lined bearing with slantwise contact are equally distributed at the shaft surface, figure 7.b and 7.c, and are between $\sigma_{ekv}=1.538\div 0.120$ MPa and $\sigma_{ekv}=0.0426\div 0.0347$ MPa, for the knots 181 and 271, and the knots 122 and 167, Table 1.

The knot 1023 was shifted the most under effect of radial force by $-1.80 \mu\text{m}$. At the very spot of the force effect on the shaft, that is at the knot 385, it shifted by $-1.70 \mu\text{m}$, figure 8.a. The extent of deformation declines to the left and to the right towards the spots 9 and 10 whose shifts at the knot 57 and 58 are $-1.20 \mu\text{m}$ $-1.30 \mu\text{m}$ respectively. At the beginning and the end of the shaft at the junction and turbine blade spot no knot shifts were recorded. The largest and the smallest knot shifts were recorded on knots 116 and 176 and they are $-1.11 \mu\text{m}$ and $-1.10 \mu\text{m}$ respectively. Shifts of the knots at the spot of the ring ball two-lined bearing with slantwise contact, figure 8.c, are in the range -1.04 to $-1.02 \mu\text{m}$ for knots 241 and 60, and -7.61 to $-7.51 \mu\text{m}$ for knots 242 and 61, Table 2.

Table 1. Results of the static analysis of the pump shaft (maximal and minimal equivalent tensions at characteristic sections)

Load variant		Loads at keypoints (MPa)				
		Beginning of the shaft	Front bearing	Rear bearing		End of the shaft
		point 2	point 7	point 12	point 13	point 16
I	Number of FE	171	281	181	122	64
	Max value	0.005	1.378	1.538	0.042	0.009
	Number of FE	231	161	271	167	245
	Min value	0.001	1.475	1.206	0.034	0.005
II	Number of FE	246	251	211	61	260
	Max value	17.975	3.823	13.467	7.943	12.134
	Number of FE	50	131	286	182	185
	Min value	1.295	0.378	2.521	0	1.007

Table 2. Results of the static analysis of the pump shaft (maximal and minimal knot shifts along the Y axes at the characteristic sections)

Load variant		Knots movement in the direction of Y- axis (μm)					
		Beginning of the shaft point 2	Front bearing point 7	Rear bearing point 12 point 13		End of the shaft point 16	
I	Max	Number of FE value	0	176	60	61	0
	Min	Number of FE value	0	-1.10	-1.02	-7.51	0
II	Max	Number of FE value	0	116	241	242	0
	Min	Number of FE value	0	-1.11	-1.04	-7.61	0
			0	0	0	0	0
			0	0	0	0	0

Under effect of the torsion moment the largest recorded equivalent tension is on the part of the shaft of $\Phi 42$ mm, at the point 3 section knot 1920, and it is $\sigma_{ekv}=24.657$ MPa. At the point 5 section the largest tension appears at knot 1357 and is $\sigma_{ekv}=15.568$ MPa. At the part of the shaft with $\Phi 40$ mm there are tensions which decrease from the point 15 towards the point 16, at the section of point 15 there was recorded the largest tension of $\sigma_{ekv}=18.584$ MPa at the knot 1667, figure 9.b. Tensions at the spot of the ring ball one-lined bearing are local, and take values at the range $\sigma_{ekv}=3.823\div 0.377$ MPa for knots 251 and 131. At the spot of the ring ball two-lined bearing with slantwise contact, the area affected by the tension is somewhat more uniform, figure 9.b with tensions (at the knots 211 and 286, and 61 and 182 resp ectively) in the range $\sigma_{ekv}=13.467\div 2.521$ MPa and $\sigma_{ekv}=7.943-0$ MPa, Table 1.

Shifting of the knots in the case of torsion moment effect on the shaft at the spot of the junction was not recorded, Table 2.

At the first case of load the maximal tension under the radial force was 9.054 MPa while in the second under the torsion moment 24.657 MPa. Based on the obtained values, it can be stated that in no characteristic section of the given shaft for no case of load, there was no of not allowed tension states, since the obtained equivalent tensions even in the most critical sections are far much smaller of the allowed ones, which for the given material is ≈ 600 MPa.

By analyzing the results of the research, it was concluded that even the largest shifts recorded under the effect of radial force of 3000 N with value of -0.0018 μm , cannot influence the plastic deformation of the shaft, while in the other case at the torsion moment no knot shifts were recorded.

5. CONCLUSION

Examination of the static behavior of the shaft by using the method of finite elements, that is the ANSYS software system, aimed for determining its static rigidity, since that is the parameter that directly influences the entire performance of the technical system.

Based on the research results of the static behavior of the centrifugal pump shaft and strain at different cross sections by using the ANSYS software, it can be concluded that working values of the load of the given shaft will not cause deterioration and shortening of usage time of the shaft, as well as the entire circuit.

REFERENCES

- [1] E. Oñate, (2009), Structural Analysis with the Finite Element Method. Linear Statics: Basis and Solids, Springer Science & Business Media. 1 (2009) p.1.
- [2] K. Čapo, D. Živojinović, The computer analysis of torsional bend spring flexure estimate, Tehnička dijagnostika. 13 (2014) 42-51.
- [3] I. Palinkaš, A. Ašonja, E. Desnica, J. Pekez, Application of computer technologies (cad/cam systems) for quality improvement of education, ANNALS of Faculty Engineering Hunedoara – International Journal of Engineering. XIV (2016) 179-184.
- [4] D. Letić, B. Davidović, B. Radulović, I. Berković, E. Desnica, The high - performance algorithm of the computer methods at the establishing of the states of stress of the brake mechanism by the finite element method (FEM), Metalurgija. 51 (2012) 513– 517.
- [5] A. Ašonja, R. Gligorić, The Calculate Analysis of Static Behaviour of Pump Shaft, Proceedings from 9th International research/expert conference - "Trends in the development of

- machinery and associated technology" (TMT 2005), 26-30 September, 2005, Antalya, Turkey.
- [6] A. Ašonja, Z. Milojević S. Navalušić, Static Behaviour Analysis of Centrifugal Pump Shaft, *Trac. and Pow. Mach.*, 9 (2004) 76-81.
- [7] A. Ašonja, E. Desnica, Research into reliability of agriculture universal joint shafts based on temperature measuring in universal joint bearing assemblies, *Span J Agric Res.* 13 (2015) 1-8.
- [8] A. Ašonja, Ž. Adamović, N. Jevtić, Analysis of Relyability of Cardan Shafts Based on Condition Diagnostics of Bearing Assembly in Cardan Joints, *Journal Metalurgia International.* 18 (2013) 216-221.
- [9] E. Desnica A. Ašonja, D. Mikić, B. Stojanović, Reliability of model of bearing assembly on an agricultural of Cardan shaft, *J. Balkan Tibological Association.* 21 (2015) 38-48.
- [10] A. Ašonja, S. Cvetković, D. Mikić, Testing of Cardan Shaft Operating Realibility in Agricultural, *Tehnička dijagnostika.* 12 (2013) 12-19.
- [11] L. Ivanović, D. Josifović, K. Živković, B. Stojanović, Cross shaft design from the aspect of capacity. *Scientific Technical Review*, 61 (2011) 56-62.
- [12] Z. Đorđević, M. Blagojević, S. Jovanović, S. Vulović, Analysis of the influence of the fibre type on static and dynamic characteristics of composite shafts, *Scientific Technical Review.* 61 (2011) 35-40.
- [13] Z. Đorđević, S. Maksimović, I. Ilić, Dynamic analysis of hybrid aluminum-composite shafts, *Scientific Technical Review*, 58 (2008), 3-7.
- [14] D. Schillinger, M. Ruess, The Finite Cell Method: A Review in the Context of Higher-Order Structural Analysis of CAD and Image-Based Geometric Models, *Arch Comput Methods Eng* 22 (2015) 391-455.
- [15] D. Letić E. Desnica B. Davidović, *AutoCAD Mechanical 2011*, Kompjuter biblioteka, Čačak, 2011, p.17.

APPENDIX: NOTATION

F_o the force in the place of the most loaded ball (N)

F_r the radial force (N)

z the total number of rolling elements of the bearing (-)

F_i the force in the place of random ball (N)

δ_i total shift in the place of rolling bodies (μm)

C_r is rigidity of one spring element ($\text{N}/\mu\text{m}$)

δ_{yi} and δ_{zi} shift components along Y and Z axes (μm)

F_{yi} and F_{zi} are shift forces along Y and Z axes (N)

C_{ru} is total radial rigidity of the bearing ($\text{N}/\mu\text{m}$)

C_{au} is total axial rigidity of the bearing ($\text{N}/\mu\text{m}$)

C_a is rigidity of one spring element ($\text{N}/\mu\text{m}$) and

C_{yi} , C_{zi} and C_{ai} rigidity of single spring elements ($\text{N}/\mu\text{m}$)